Hepcidin-Induced Endocytosis of Ferroportin Is Dependent on Ferroportin Ubiquitination

Bo Qiao,[1] Priscilla Sugianto,[1] Eileen Fung,[1] Alejandro del-Castillo-Rueda,[3] Maria-Josefa Moran-Jimenez,[4]
Tomas Ganz,[1,2] and Elizabeta Nemeth[1,*]
[1]Department of Medicine
[2]Department of Pathology
David Geffen School of Medicine, University of California, Los Angeles, Los Angeles, CA 90095, USA
[3]Unidad de Ferropatologia, Departamento de Medicina Interna, Hospital General Universitario Gregorio Maranon, Facultad de Medicina,
Universidad Complutense, 28007 Madrid, Spain
[4]Centro de Investigacion, Instituto de Investigacion Hospital 12 de Octubre, 28041 Madrid, Spain
*Correspondence: enemeth@mednet.ucla.edu
DOI 10.1016/j.cmet.2012.03.018

SUMMARY

Ferroportin exports iron into plasma from absorptive enterocytes, erythrophagocytosing macrophages, and hepatic stores. The hormone hepcidin controls cellular iron export and plasma iron concentrations by binding to ferroportin and causing its internalization and degradation. We explored the mechanism of hepcidin-induced endocytosis of ferroportin, the key molecular event in systemic iron homeostasis. Hepcidin binding caused rapid ubiquitination of ferroportin in cell lines overexpressing ferroportin and in murine bone marrow-derived macrophages. No hepcidin-dependent ubiquitination was observed in C326S ferroportin mutant which does not bind hepcidin. Substitutions of lysines between residues 229 and 269 in the third cytoplasmic loop of ferroportin prevented hepcidin-dependent ubiquitination and endocytosis of ferroportin, and promoted cellular iron export even in the presence of hepcidin. The human ferroportin mutation K240E, previously associated with clinical iron overload, caused hepcidin resistance in vitro by interfering with ferroportin ubiquitination. Our study demonstrates that ubiquitination is the functionally relevant signal for hepcidin-induced ferroportin endocytosis.

INTRODUCTION

Hepcidin-induced ferroportin internalization is a critical event in iron homeostasis. Ferroportin (Fpn) is a conserved iron exporter expressed in tissues supplying iron to plasma, including duodenal enterocytes absorbing dietary iron and macrophages recycling iron from old erythrocytes (Donovan et al., 2005). The rate of iron export is determined by the concentration of Fpn on the plasma membranes of iron-exporting cells. Hepcidin binds to Fpn and causes its endocytosis and degradation, thereby regulating iron efflux (Nemeth et al., 2004). Alterations in hepcidin or Fpn production, or in their interaction, cause iron

overload diseases and iron-restricted anemias (Ganz and Nemeth, 2011). The mechanism by which hepcidin induces Fpn endocytosis is therefore of great interest not only as fundamental iron physiology but also for developing drug leads.

In general, ligand-induced endocytosis of transporters and receptors is triggered by a conformational change followed by phosphorylation and/or ubiquitination of their cytoplasmic segments (Bonifacino and Traub, 2003). The internalization of Fpn was reported to be initiated by ligand-induced phosphorylation on Y302/Y303 residues by JAK2 kinase (De Domenico et al., 2007, 2009). Despite extensive efforts, we and others (Ross et al., 2012 [this issue of *Cell Metabolism*]) have not observed any evidence of Fpn phosphorylation or involvement of JAK2 in Fpn endocytosis. We therefore re-examined the mechanisms for hepcidin-induced Fpn endocytosis.

RESULTS AND DISCUSSION

Hepcidin Binding Triggers Rapid Ubiquitination of Fpn

HEK293 cells stably expressing doxycycline (Dox)-inducible human Fpn-GFP were treated with hepcidin, and lysates were immunoprecipitated with an anti-GFP antibody (Ab) and immunoblotted with an anti-ubiquitin (Ub) Ab recognizing both poly- and monoUb (FK2). Fpn-GFP ubiquitination was detected within 10 min after hepcidin treatment and lasted for at least 2 hr (Figure 1A). Human Fpn-GFP protein is ~90 kDa, and each Ub molecule is ~8.5 kDa. The major ubiquitinated species of Fpn-GFP migrated in SDS-PAGE with an apparent mass of ~130–180 kDa and so may contain 4–10 Ub molecules, whereas higher-mass species (~250–300 kDa) may contain up to 20–25 Ubs. To distinguish between polyubiquitination and multimonoubiquitination (Figure 1B), we used an Ab recognizing polyUb only (FK1). FK1 Ab showed a similar pattern of reactivity as the FK2 Ab, demonstrating that Fpn-GFP was at least polyubiquitinated, but we could not rule out that Fpn may also be mono- or multimonoubiquitinated. All subsequent Ub blots in the manuscript were probed with the FK2 Ab. Hepcidin also triggered rapid and dose-dependent Fpn-GFP ubiquitination in HEK293 cells expressing ponasterone (Pon)-inducible mouse Fpn-GFP (see Figures S1A and S1B online). Ubiquitination of Fpn was not an artifact of overexpression, as hepcidin also induced strong and rapid (within 5 min) ubiquitination of endogenous
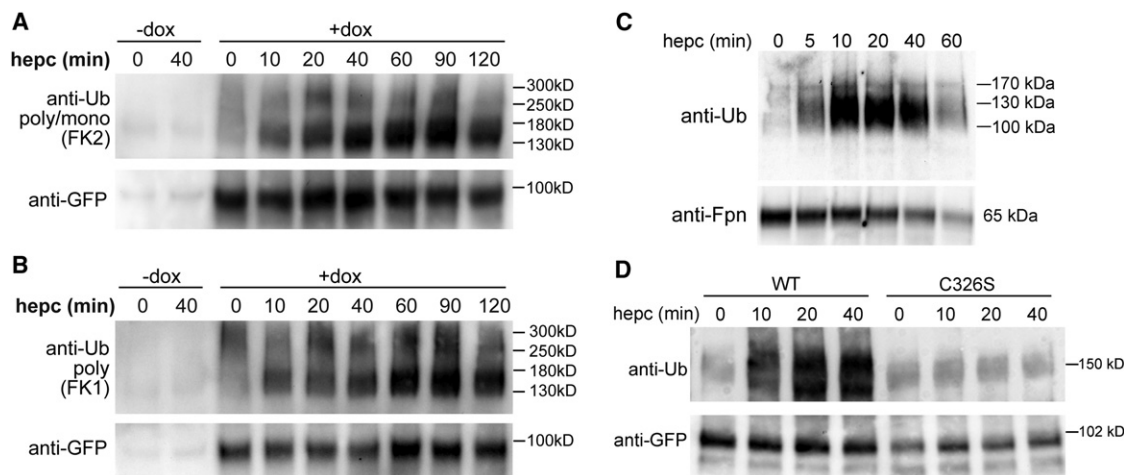
Figure 1. Hepcidin Binding Causes Rapid Ubiquitination of Fpn

(A) HEK293 cells stably transfected with a Dox-inducible human Fpn-GFP were either not induced (−dox) or induced (+dox) to express Fpn-GFP, then treated with 1 μg/ml (360 nM) hepcidin for up to 2 hr. Cell lysates were immunoprecipitated with anti-GFP Ab (ab6556) and blotted with anti-poly/monoUb Ab (FK2). The blot was reprobed with a different anti-GFP Ab (7.1/13.1) to confirm even loading.

(B) Cells were treated identically to those in (A), but the blot was incubated with an Ab recognizing polyUb only (FK1).

(C) Mouse primary bone marrow-derived macrophages were treated with 1 μg/ml hepcidin for up to 1 hr. Lysates were immunoprecipitated with anti-Fpn Ab (MTP11-A) and immunoblotted with FK2 anti-poly/monoUb Ab. The amount of immunoprecipitated Fpn was verified by probing the blot with another anti-mouse Fpn Ab (R1).

(D) HEK293 cells stably expressing Dox-inducible WT Fpn-GFP or C326S mutant which does not bind hepcidin were treated with 1 μg/ml hepcidin and processed as in (A).

Fpn in mouse primary bone marrow-derived macrophages (BMDMs) (Figure 1C). The apparent mass of Fpn in BMDMs is ∼65 kDa, whereas ubiquitinated species were about ∼100–150 kDa, indicating the attachment ∼4–10 Ub molecules, similar to overexpressing cell lines.

No hepcidin-dependent ubiquitination was observed in cells stably expressing an inducible C326S Fpn-GFP mutant which does not bind hepcidin (Fernandes et al., 2009) (Figure 1D). The result demonstrated that direct interaction between hepcidin and Fpn is required for Fpn ubiquitination.

Inhibition of Ubiquitination Prevents Fpn Internalization

Ubiquitination is catalyzed by the sequential action of three enzymes: E1, E2, and E3. We used PYR-41, an inhibitor of the Ub-activating enzyme E1, to examine whether blocking ubiquitination interferes with Fpn internalization. Throughout the study, the terms "internalization" or "endocytosis" refer to net endocytosis, i.e., detectable redistribution of Fpn from the cell surface to intracellular compartments. The E1 inhibitor prevented Fpn endocytosis when it was added together with hepcidin (Figure S2A). Western blotting with anti-Ub Ab confirmed that the E1 inhibitor decreased Fpn-GFP ubiquitination (Figure S2B). These results suggested that Fpn ubiquitination is necessary for its internalization by hepcidin.

Identification of Fpn Residues Involved in Ubiquitination

To determine which Fpn residues undergo functionally important ubiquitination, we performed site-directed mutagenesis of Fpn focusing on regions rich in lysine, the most commonly ubiquitinated amino acid. Human Fpn is thought to have a total of 14 or 15 cytoplasmic lysines (Liu et al., 2005; Rice et al., 2009),

with our previous study (Preza et al., 2011) supporting the model with 14 lysines. Most of the lysines are located in the third intracellular loop (seven or eight lysines, K225 or K229 through K269) and the C-terminal cytoplasmic segment (three lysines, K549, K558, and K562) (Figure S3A). The remaining lysines are in the first (K85, K90), second (K169), and fourth intracellular loops (K366). Because membrane receptors and transport proteins are usually ubiquitinated on multiple lysines (Mollah et al., 2007; Wu et al., 2010; Miranda and Sorkin, 2007), we focused on the third Fpn intracellular loop and the C terminus. We first scanned for larger regions involved in ubiquitination by deleting residues 229–269, 225–247, 247–269, or 549–562. Although large deletions could alter Fpn-GFP synthesis, localization, or hepcidin binding, we argued that if hepcidin-induced endocytosis was preserved in any of the mutants, it would allow us to omit the region from detailed mutagenesis. We transfected the mutants into HEK293 cells and examined the response to hepcidin by fluorescent microscopy (Figure S3B). Deletion 549–562 did not interfere with hepcidin-mediated Fpn internalization, but the deletions in the third intracellular loop did (229–269, 225–247, and partially 247–269). The latter also affected trafficking of Fpn-GFP to the membrane. We then performed less disruptive mutagenesis of the third intracellular loop by substituting multiple lysines with arginines. The specific combinations of substitutions were chosen to accommodate the requirement in multisite-directed mutagenesis for nonoverlapping mutagenesis primers. In transiently transfected HEK293 cells, the K229R/K247R/K269R Fpn-GFP mutant was partially resistant to hepcidin-mediated internalization (Figure S3B), and K225R/K240R/K258R and K240/258R mutants were strongly resistant.
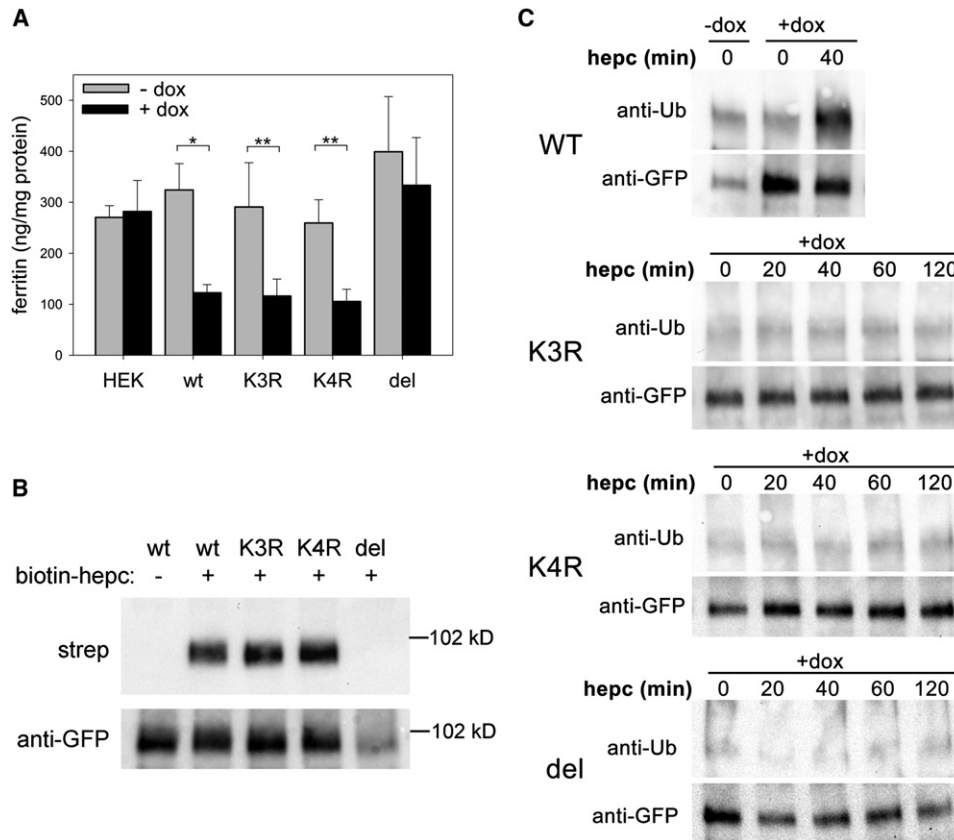
Figure 2. Lysine Substitutions in the Third Intracellular Loop of Fpn Prevent Hepcidin-Dependent Ubiquitination of Fpn without Affecting Iron-Exporting Function or Hepcidin Binding

(A) Untransfected HEK293 cells (HEK) and HEK293 stably transfected with Dox-inducible K3R (K229R/K240R/K247R), K4R (K229R/K240R/K247R/K258R), or DEL (del229–269) Fpn-GFP mutant were incubated without (−dox) or with 0.5 μg/ml dox (+dox). After 24 hr, protein lysates were assayed for ferritin levels. Vertical bars and error bars represent the mean and standard deviation of four to seven experiments. *p = 0.001, **p < 0.001 by t test.

(B) Cells were induced with Dox and treated with 10 μg/ml (3.6 μM) biotinylated hepcidin for 30 min. Protein lysates were immunoprecipitated with anti-GFP Ab (ab290), and biotinylated hepcidin bound to Fpn-GFP was detected with streptavidin-HRP. The amount of immunoprecipitated Fpn-GFP was determined by western blotting with anti-GFP Ab (7.1/13.1).

(C) Cells were induced with Dox to express WT or mutant Fpn-GFP and treated with 1 μg/ml hepcidin for up to 2 hr. Protein lysates were immunoprecipitated with anti-GFP Ab (ab6556) and immunoblotted with anti-poly/monoUb Ab (FK2) or anti-GFP Ab (7.1/13.1).

Residue K253 was previously reported to be essential for Fpn ubiquitination, but this ubiquitination was described as important only for Fpn degradation, not internalization (De Domenico et al., 2007, 2011). We generated a Fpn-GFP mutant that contained the K253R substitution (K236R/K253R) and examined its ubiquitination after treatment with hepcidin. In contrast to the published study (De Domenico et al., 2007), the K236R/K253R mutant was ubiquitinated similarly to WT Fpn-GFP (Figure S4), indicating that the K253 residue is not the predominant site for Fpn ubiquitination. Accordingly, the K236R/K253R mutant internalized normally after hepcidin treatment (Figure S3B).

Analysis of Stably Transfected Lysine Mutants

Transient transfection of cells with Fpn constructs is a suboptimal approach for the study of Fpn function and response to hepcidin because of the uncontrolled expression of Fpn and cell-to-cell variability in transfection efficiency. We therefore generated stably transfected HEK293 cells expressing inducible human Fpn-GFP (K3R [K229R/K240R/K247R] and K4R [K229R/

K240R/K247R/K258R]) or the 229–269 deletion. The K2R mutant (K240R/K258R) was generated and analyzed independently in the companion study (Ross et al., 2012). We did not attempt to mutagenize every lysine in the cytoplasmic Fpn segments, because the large number of intracellular lysines made the analysis of possible combinations impractical. Moreover, several studies indicate that when major lysine sites are mutated, it can force the ubiquitination of other lysines (Miranda and Sorkin, 2007). Thus, our approach in studying Fpn ubiquitination does not exclude the possibility that additional cytoplasmic lysines are important in ubiquitination, but it provides proof-of-principle evidence for the role of ubiquitination in Fpn internalization by hepcidin.

We first assessed the iron-exporting function of the stably transfected Dox-inducible Fpn-GFP mutants by measuring ferritin as a marker of intracellular iron. Cells expressing K3R or K4R mutants were iron depleted similarly to wild-type Fpn-GFP (Figure 2A), indicating that lysine substitutions did not alter the mutants' iron-exporting function or plasma membrane
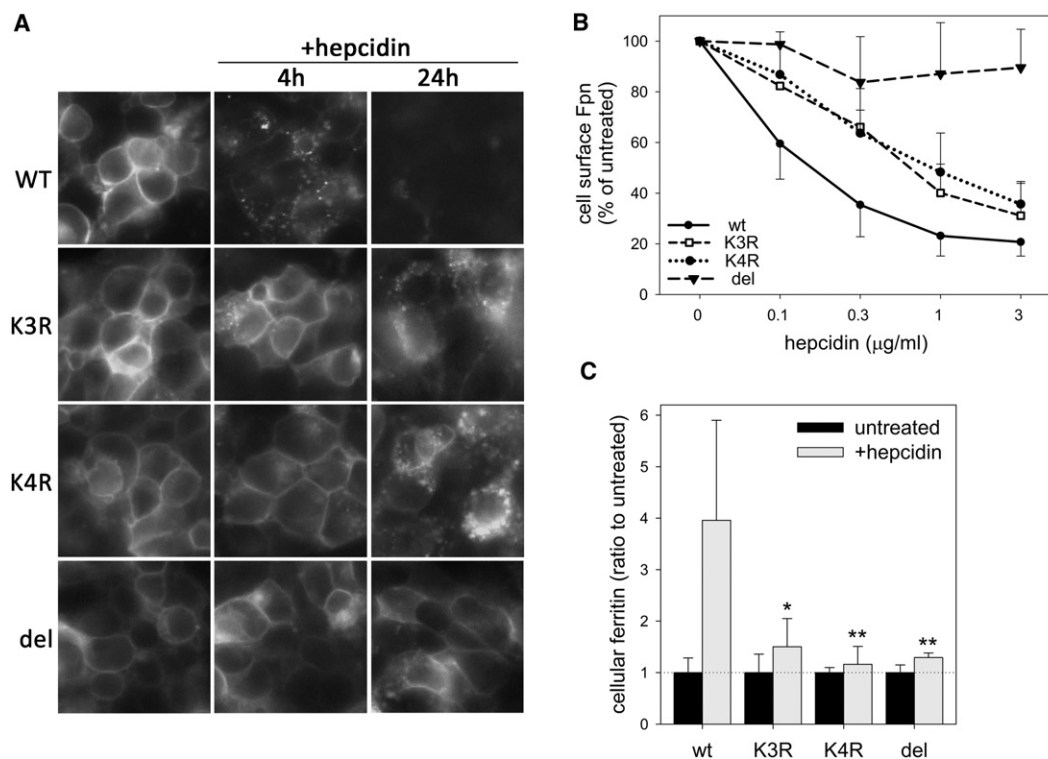
Figure 3. Lysine Substitutions in the Third Intracellular Loop of Fpn Interfere with Hepcidin-Induced Fpn Endocytosis and Cellular Iron Retention

Stably transfected HEK293 cells were induced with Dox to express WT, K3R, K4R, or del229–269 Fpn-GFP. Dox was washed off prior to adding hepcidin.

(A) Cells were treated with 1 µg/ml (360 nM) hepcidin and Fpn-GFP location assessed at 4 and 24 hr by fluorescent microscopy.

(B) Cells were treated with indicated hepcidin concentrations. After 4 hr, cell surface Fpn was detected by staining with anti-human Fpn Ab against an extracellular loop of Fpn (M1), followed by the secondary Ab conjugated to PE. Fluorescence was quantified by flow cytometry and expressed as percentage fluorescence of untreated samples. Each point represents the mean and standard deviation of three independent experiments. Each of the mutant curves (K3R, K4R, or DEL) significantly differed from the WT ($p < 0.001$, two-way ANOVA).

(C) Cells expressing WT or mutant Fpn-GFP were incubated without or with 0.2 µg/ml (72 nM) hepcidin for 24 hr. Cell lysates were assayed for ferritin. Fold increase in ferritin after hepcidin treatment is shown as a mean and standard deviation of at least six separate measurements. *$p = 0.003$ and **$p = 0.001$ by Mann-Whitney rank sum test for the comparison of the hepcidin-treated mutant with the hepcidin-treated WT cells. For K3R, K4R, or DEL mutants, no significant difference in ferritin levels was observed between hepcidin-treated or untreated cells.

location. Although Dox can chelate metals including iron, Dox treatment of untransfected HEK293 cells under the conditions and dose used (0.5 µg/ml) did not cause a measurable change in cellular iron, as reflected in ferritin levels. The 229–269 deletion abolished iron export, indicating a disruptive conformational change or loss of specific residues necessary for the iron-exporting function of Fpn.

Hepcidin binding to Fpn depends on several residues in the extracellular loop 323–343 (Preza et al., 2011). In principle, deletions or substitutions we made could cause hepcidin resistance not only by decreasing ubiquitination but also by altering the conformation of the hepcidin-binding loop. To evaluate hepcidin binding to mutant Fpns, cells were treated with N-terminally biotinylated hepcidin, and its association with Fpn-GFP was determined by far-western blotting with streptavidin. Biotinylated hepcidin bound to and migrated with WT Fpn-GFP as expected (Figure 2B). K3R and K4R Fpn-GFP bound hepcidin similarly to WT. Hepcidin binding by del229–269 Fpn-GFP was undetectable. We used the del229–269 mutant in subsequent experiments as a noninternalizing Fpn-GFP control.

In contrast to WT Fpn-GFP, hepcidin-dependent ubiquitination was not observed in any of the mutant Fpns (K3R, K4R and del229–269) within 2 hr after hepcidin treatment (Figure 2C). Given that K3R and K4R mutants bind hepcidin normally, some or all of the lysines that were substituted in these mutants are required for Fpn ubiquitination.

Ubiquitination of Lysines in the Third Intracellular Loop of Fpn Is Required for Hepcidin-Induced Fpn Internalization

We next examined the endocytosis of K3R, K4R, and del229–269 Fpn mutants after treatment with hepcidin. Fluorescent microscopy showed that, in contrast to WT Fpn-GFP which internalized readily upon hepcidin addition, K3R and K4R mutants remained at the cell surface at 4 hr (Figure 3A). After 24 hr, these mutants underwent partial internalization and degradation but much less than WT Fpn-GFP. The partial endocytosis suggests that additional lysine residues may become ubiquitinated, or another mechanism becomes important. Del229–269 mutant had mostly plasma membrane localization even after 24 hr.
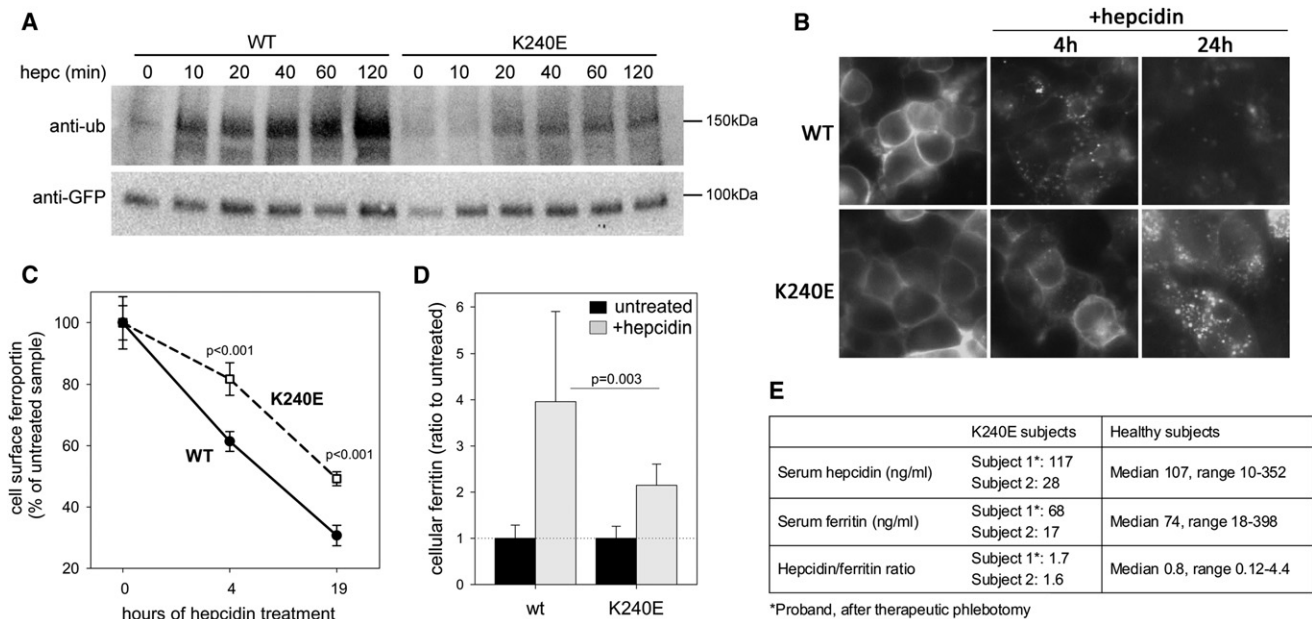
Figure 4. K240E Human Fpn Mutation Causes Hepcidin Resistance

(A) Stably transfected HEK293 cells were induced with Dox to express WT or K240E Fpn-GFP and were treated with 1 μg/ml hepcidin for up to 2 hr. Protein lysates were immunoprecipitated with anti-GFP Ab (ab6556) and immunoblotted with anti-poly/monoUb Ab (FK2) or anti-GFP Ab (7.1/13.1).

(B) HEK293 cells induced to express WT or K240E Fpn-GFP were treated with 1 μg/ml hepcidin and Fpn-GFP location assessed after 4 and 24 hr by fluorescent microscopy. WT images are identical to those in Figure 3A.

(C) HEK293 cells induced to express WT or K240E Fpn-GFP were treated with 0.2 μg/ml hepcidin for the indicated time. To quantify cell surface Fpn, cells were stained with anti-human Fpn Ab against an extracellular loop of Fpn (M1), followed by the secondary Ab conjugated to PE. Fluorescence was measured by flow cytometry and results expressed as percentage of the fluorescence of untreated samples. Means and standard deviations of four separate measurements are shown. K240E and WT were compared at each time point by t test.

(D) Cells expressing WT or K240E Fpn-GFP were incubated without or with 0.2 μg/ml hepcidin for 24 hr, and protein lysates were assayed for ferritin (n = 10 for WT and 12 for K240E). WT values are the same as in Figure 3C. The means and standard deviations of fold increase in ferritin levels after hepcidin treatment are shown, p = 0.003 by Mann-Whitney rank sum test for the comparison of the hepcidin-treated K240E with the hepcidin-treated WT cells.

(E) Shown is serum hepcidin, ferritin, and hepcidin/ferritin ratio in two subjects with K240E mutation, compared to historical controls (Ganz et al., 2008).

We also quantified the endocytosis of Fpn mutants as a function of increasing hepcidin concentration using flow cytometry of live cells stained with an Ab to an extracellular Fpn loop (M1). Hepcidin caused an expected dose-dependent decrease in cell surface WT Fpn-GFP (Figure 3B), whereas K3R and K4R mutations interfered with Fpn-GFP internalization, particularly at lower hepcidin concentrations (p < 0.001 for each mutant versus WT by two-way ANOVA). As expected, del229–269 was completely resistant to internalization.

Decreased internalization of Fpn should allow greater cellular iron export. Indeed, measurement of intracellular ferritin concentrations showed that in contrast to the iron retention in hepcidin-treated cells expressing WT Fpn-GFP, K3R and K4R Fpn-GFP continued exporting iron in the presence of hepcidin (Figure 3C).

The results confirmed the importance of lysine residues in segment 229–269 for hepcidin-mediated Fpn internalization. The specific details of Fpn endocytic sorting, including which Ub-binding adaptor proteins may be involved, remain to be determined.

K240E Substitution in Humans: A Case of Hepcidin Resistance?

A patient with mild iron overload was reported to be heterozygous for two mutations, c.-20G > A in *HFE* and p.K240E in Fpn (Del-Castillo-Rueda et al., 2011), and we hypothesized that K240E substitution could be causing ferroportin resistance to hepcidin. We examined the effect of K240E substitution in vitro in stably transfected HEK293 cells expressing Dox-inducible K240E Fpn-GFP. In comparison to WT Fpn-GFP, ubiquitination of K240E mutant was considerably diminished (Figure 4A). The mutant also had a defect in hepcidin-induced endocytosis. Fluorescent microscopy 4 hr after hepcidin addition revealed that more K240E Fpn-GFP protein remained on the cell surface compared to WT (Figure 4B), and at 24 hr the K240E mutant was less degraded than WT Fpn-GFP. Quantitation of cell surface Fpn by flow cytometry confirmed the delay in hepcidin-induced endocytosis of K240E Fpn-GFP (Figure 4C). Furthermore, as assessed by ferritin assay, cells expressing K240E Fpn-GFP were partially resistant to hepcidin-mediated iron retention (Figure 4D). Thus, decreased hepcidin-mediated ubiquitination and decreased endocytosis of Fpn due to K240E substitution could cause partial resistance to hepcidin and mild iron overload. Unlike patients with HFE mutations (Piperno et al., 2007), the proband shows features of resistance to hepcidin, with hepcidin levels that were above the median hepcidin concentration of healthy historical controls (Ganz et al., 2008), and a normal hepcidin/ferritin ratio (Figure 4E). His daughter, also heterozygous for the K240E

substitution, had no signs of iron loading, but this is not unusual for young women even when carrying hemochromatosis-causing mutations (Laine et al., 2005). We therefore propose that the mild iron overload in the proband could result from the effect of K240E substitution on ferroportin internalization by hepcidin.

Several other human mutations have been reported in the third intracellular loop of Fpn. D270V (Zaahl et al., 2004) was associated with mild clinical iron overload and phenotype resembling hepcidin resistance (elevated transferrin saturation and serum iron), whereas G267D (Cremonesi et al., 2005) and polymorphism Q248H (Gordeuk et al., 2003) were associated with elevated serum ferritin but normal serum iron, similar to classical Fpn disease due to loss of Fpn function. Because amino acids proximal to lysine residues are critical for controlling the efficiency of lysine ubiquitination (Sadowski and Sarcevic, 2010), it is possible that these mutations could cause iron disturbances by decreasing or increasing the efficiency of Fpn ubiquitination.

Conclusions

Molecular mechanism of hepcidin-mediated Fpn endocytosis was previously reported to involve phosphorylation of Y302/Y303 residues by JAK2 kinase (De Domenico et al., 2007, 2009). However, together with the companion study by Ross et al. (2012), we now provide a comprehensive revision of the mechanism of hepcidin-induced Fpn endocytosis. Although we used reagents and experimental setup similar to those of De Domenico et al., including Pon-inducible mouse WT Fpn-GFP cell line (Nemeth et al., 2004) and transient transfection of Fpn-GFP mutants into HEK293 cells, we were unable to reproduce their previously reported findings. We also verified the effects of Fpn mutations in stably transfected cells expressing Dox-inducible mutants, a system in which the effects of mutations are less confounded by cell-to-cell variability than in transient transfections. The discrepancy in the results will require further investigation.

Ross et al. (2012) demonstrated that Fpn is not phosphorylated after hepcidin binding, and that neither Y302/Y303 residues nor JAK2 is necessary for Fpn internalization. Our study instead showed that ubiquitination is the signal required for Fpn endocytosis after hepcidin binding. Hepcidin triggered Fpn polyubiquitination in cells overexpressing Fpn-GFP (both Pon- and Dox-inducible) as well as in primary mouse BMDMs. Substitutions of lysines in the third intracellular loop of Fpn ablated ubiquitination, greatly retarded hepcidin-induced Fpn endocytosis, and promoted cellular iron export despite the presence of hepcidin. It is not yet clear whether the observed pattern of Fpn ubiquitination also directs Fpn trafficking to lysosomes where Fpn is degraded (Nemeth et al., 2004).

The hepcidin-Fpn axis plays a pathogenic role in multiple iron disorders. Thus, modulating Fpn internalization is a potential therapeutic target. Ubiquitination, however, regulates a broad spectrum of biological processes, and the feasibility of any pharmacological interventions would depend on achieving high target specificity, perhaps by generating specific inhibitors of the E3 ubiquitin ligase(s) involved in Fpn endocytosis. More detailed examination of the molecular mechanisms regulating Fpn ubiquitination and endocytosis is therefore warranted.

EXPERIMENTAL PROCEDURES

Site-Directed Mutagenesis

Human Fpn-GFP in pGFP-N3 vector (Fernandes et al., 2009) was used as the template for site-directed mutagenesis. Deletions, single mutations, or multiple mutations were introduced using QuikChange II XL and Lightning Multi Site-Directed Mutagenesis kits (Agilent Technologies, Santa Clara, CA) and confirmed by sequencing. Mutagenesis primers are listed in Table S1.

Transient Transfection and Microscopy

Fpn-GFP plasmids were transiently transfected into HEK293T cells using either Lipofectamine 2000 (Invitrogen, Carlsbad CA) or Amaxa nucleofection (Lonza, Walkersville, MD). In transiently transfected cells, the endocytic effect of hepcidin on Fpn can be obscured by the continuous high rate of Fpn-GFP production. Therefore, cells were treated with 50 μg/ml cycloheximide for 2 hr to slow down Fpn-GFP synthesis before hepcidin addition. Cells were visualized with an epifluorescence microscope (Nikon Eclipse, Melville, NY), and images were acquired with a 40× objective, SPOT camera, and SPOT Advanced Imaging Software (Diagnostic Instruments, Sterling Heights, MI).

Stably Transfected Cell Lines

Human WT and mutant K3R, K4R, K240E, del229–269, and C326S Fpn-GFP constructs were cloned into pLVX-Tight-Puro lentiviral vector (Clontech, Mountain View, CA) and verified by sequencing. Following viral packaging (UCLA Vector Core facility), Tet-on Advanced HEK293 cells (Clontech) were infected, and colonies were selected in the presence of 3 μg/ml puromycin and 100 μg/ml G418 for 3 weeks. Dox (Sigma, St. Louis, MO) was used to induce expression of Fpn-GFP. For some experiments, we also used HEK293 cells expressing Pon-inducible mouse Fpn-GFP (Nemeth et al., 2004). Hepcidin was purchased from Peptides International (Louisville, KY) and E1 enzyme inhibitor PYR-41 from Calbiochem (San Diego, CA).

Primary Murine Macrophage Culture

BMDMs were isolated from mouse femurs and grown in DMEM with 10% heat-inactivated fetal calf serum and 20% L-cell-conditioned medium for 7 days. To increase endogenous Fpn, cells were incubated with Fe-NTA (100 μM $FeCl_3$, 400 μM NTA) for 20 hr. Animal studies were approved by the UCLA Animal Research Committee.

Immunoprecipitation and Western Blotting

Proteins were extracted with RIPA buffer supplemented with protease inhibitor cocktail. Fpn-GFP was immunoprecipitated with anti-GFP rabbit polyclonal Ab (ab6556 or ab290, Abcam, Cambridge, MA) and endogenous BMDM Fpn with anti-mouse Fpn antibody (MTP-11A, ADI, San Antonio, TX). For western blotting, primary antibodies included the following: anti-Ub monoclonal antibodies FK1 and FK2 (Enzo Life Sciences, Farmingdale, NY), both at 1 μg/ml final concentration; anti-GFP mouse monoclonal antibody (0.4 μg/ml, clones 7.1/13.1, Roche, Indianapolis, IN); and rat anti-mouse Fpn antibody (1–2 μg/ml R1, Ab description provided in the Supplement). Chemiluminescent signal was detected using ChemiDoc XRS+ System with Image Lab Software (Bio-Rad).

Hepcidin Binding Assay

Cells were treated with 10 μg/ml N-terminally biotinylated hepcidin (Peptides International) for 30 min at 37C. Protein lysates were immunoprecipitated with anti-GFP Ab and blotted with Streptavidin-HRP (Pierce, Rockford, IL).

Ferritin Assay

Cellular ferritin was assayed by ferritin ELISA (Ramco Laboratories, Stafford, TX) and normalized to the total protein concentration in each sample, as determined by the BCA assay.

Flow Cytometry

Fpn-GFP cell lines were induced with Dox and treated with hepcidin. Cells were then detached with TrypLE (Invitrogen), incubated with primary antibody

against Fpn extracellular loop (mouse anti-human Fpn antibody M1, Amgen, Ross et al., [2012] companion manuscript), and secondary antibody conjugated to PE. Fluorescence was quantified by flow cytometry at UCLA Jonsson Comprehensive Cancer Center and Center for AIDS Research Flow Cytometry Core Facility.

Serum Hepcidin and Ferritin Measurement

Serum hepcidin was measured by competitive ELISA at Intrinsic LifeSciences LLC (Ganz et al., 2008), and serum ferritin was measured by the Clinical Laboratory at Hospital General Universitario Gregorio Maranon.

Statistical Analysis

Statistical analysis employed the t test (normally distributed data), Mann-Whitney rank sum test (data with nonnormal distribution), and two-way ANOVA (comparison of groups) (SigmaPlot version 11.0, Systat Software). The error bars in the figures represent standard deviations of the indicated number of experiments.

SUPPLEMENTAL INFORMATION

Supplemental Information includes four figures, one table, Supplemental Experimental Procedures, and Supplemental References and can be found with this article at doi:10.1016/j.cmet.2012.03.018.

REFERENCES

Bonifacino, J.S., and Traub, L.M. (2003). Signals for sorting of transmembrane proteins to endosomes and lysosomes. Annu. Rev. Biochem. 72, 395–447.

Cremonesi, L., Forni, G.L., Soriani, N., Lamagna, M., Fermo, I., Daraio, F., Galli, A., Pietra, D., Malcovati, L., Ferrari, M., et al. (2005). Genetic and clinical heterogeneity of ferroportin disease. Br. J. Haematol. 131, 663–670.

De Domenico, I., Ward, D.M., Langelier, C., Vaughn, M.B., Nemeth, E., Sundquist, W.I., Ganz, T., Musci, G., and Kaplan, J. (2007). The molecular mechanism of hepcidin-mediated ferroportin down-regulation. Mol. Biol. Cell 18, 2569–2578.

De Domenico, I., Lo, E., Ward, D.M., and Kaplan, J. (2009). Hepcidin-induced internalization of ferroportin requires binding and cooperative interaction with Jak2. Proc. Natl. Acad. Sci. USA 106, 3800–3805.

De Domenico, I., Lo, E., Yang, B., Korolnek, T., Hamza, I., Ward, D.M., and Kaplan, J. (2011). The role of ubiquitination in hepcidin-independent and hepcidin-dependent degradation of ferroportin. Cell Metab. 14, 635–646.

Del-Castillo-Rueda, A., Moreno-Carralero, M.I., Alvarez-Sala-Walther, L.A., Cuadrado-Grande, N., Enriquez-de-Salamanca, R., Mendez, M., and Moran-Jimenez, M.J. (2011). Two novel mutations in the SLC40A1 and HFE genes implicated in iron overload in a Spanish man. Eur. J. Haematol. 86, 260–264.

Donovan, A., Lima, C.A., Pinkus, J.L., Pinkus, G.S., Zon, L.I., Robine, S., and Andrews, N.C. (2005). The iron exporter ferroportin/Slc40a1 is essential for iron homeostasis. Cell Metab. 1, 191–200.

Fernandes, A., Preza, G.C., Phung, Y., De Domenico, I., Kaplan, J., Ganz, T., and Nemeth, E. (2009). The molecular basis of hepcidin-resistant hereditary hemochromatosis. Blood 114, 437–443.

Ganz, T., and Nemeth, E. (2011). Hepcidin and disorders of iron metabolism. Annu. Rev. Med. 62, 347–360.

Ganz, T., Olbina, G., Girelli, D., Nemeth, E., and Westerman, M. (2008). Immunoassay for human serum hepcidin. Blood 112, 4292–4297.

Gordeuk, V.R., Caleffi, A., Corradini, E., Ferrara, F., Jones, R.A., Castro, O., Onyekwere, O., Kittles, R., Pignatti, E., Montosi, G., et al. (2003). Iron overload in Africans and African-Americans and a common mutation in the SCL40A1 (ferroportin 1) gene. Blood Cells Mol. Dis. 31, 299–304.

Laine, F., Jouannolle, A.M., Morcet, J., Brigand, A., Pouchard, M., Lafraise, B., Mosser, J., David, V., and Deugnier, Y. (2005). Phenotypic expression in detected C282Y homozygous women depends on body mass index. J. Hepatol. 43, 1055–1059.

Liu, X.B., Yang, F., and Haile, D.J. (2005). Functional consequences of ferroportin 1 mutations. Blood Cells Mol. Dis. 35, 33–46.

Miranda, M., and Sorkin, A. (2007). Regulation of receptors and transporters by ubiquitination: new insights into surprisingly similar mechanisms. Mol. Interv. 7, 157–167.

Mollah, S., Wertz, I.E., Phung, Q., Arnott, D., Dixit, V.M., and Lill, J.R. (2007). Targeted mass spectrometric strategy for global mapping of ubiquitination on proteins. Rapid Commun. Mass Spectrom. 21, 3357–3364.

Nemeth, E., Tuttle, M.S., Powelson, J., Vaughn, M.B., Donovan, A., Ward, D.M., Ganz, T., and Kaplan, J. (2004). Hepcidin regulates cellular iron efflux by binding to ferroportin and inducing its internalization. Science 306, 2090–2093.

Piperno, A., Girelli, D., Nemeth, E., Trombini, P., Bozzini, C., Poggiali, E., Phung, Y., Ganz, T., and Camaschella, C. (2007). Blunted hepcidin response to oral iron challenge in HFE-related hemochromatosis. Blood 110, 4096–4100.

Preza, G.C., Ruchala, P., Pinon, R., Ramos, E., Qiao, B., Peralta, M.A., Sharma, S., Waring, A., Ganz, T., and Nemeth, E. (2011). Minihepcidins are rationally designed small peptides that mimic hepcidin activity in mice and may be useful for the treatment of iron overload. J. Clin. Invest. 121, 4880–4888.

Rice, A.E., Mendez, M.J., Hokanson, C.A., Rees, D.C., and Bjorkman, P.J. (2009). Investigation of the biophysical and cell biological properties of ferroportin, a multipass integral membrane protein iron exporter. J. Mol. Biol. 386, 717–732.

Ross, S.L., Tran, L., Winters, A., Lee, K.-J., Plewa, C., Foltz, I., King, C., Miranda, L.P., Allen, J., Beckman, H., et al. (2012). Molecular mechanism of hepcidin-mediated ferroportin internalization requires ferroportin lysines, not tyrosines or JAK-STAT. Cell Met. 15, this issue, 905–917.

Sadowski, M., and Sarcevic, B. (2010). Mechanisms of mono- and poly-ubiquitination: ubiquitination specificity depends on compatibility between the E2 catalytic core and amino acid residues proximal to the lysine. Cell Div. 5, 19. 10.1186/1747-1028-5-19.

Wu, T., Merbl, Y., Huo, Y., Gallop, J.L., Tzur, A., and Kirschner, M.W. (2010). UBE2S drives elongation of K11-linked ubiquitin chains by the anaphase-promoting complex. Proc. Natl. Acad. Sci. USA 107, 1355–1360.

Zaahl, M.G., Merryweather-Clarke, A.T., Kotze, M.J., van der Merwe, S., Warnich, L., and Robson, K.J. (2004). Analysis of genes implicated in iron regulation in individuals presenting with primary iron overload. Hum. Genet. 115, 409–417.